12-2020

Stability of Group Four Monochalcogenides in Water and Air

William Shattuck
University of Arkansas, Fayetteville

Stability of Group Four Monochalcogenides in Water and Air

A thesis submitted in partial fulfillment
of the requirements for the degree of
Master of Science in Physics

by

William Shattuck
University of Arkansas
Bachelor of Science in Physics, 2018

December 2020
University of Arkansas

This thesis is approved for recommendation to the Graduate Council.

Hugh O. H. Churchill, PhD
Thesis Director

Woodrow Shew, PhD
Committee Member

Julio R. Gea-Banacloche, PhD
Committee Member

Abstract

Previously published works have simulated the behavior of monolayer group IV monochalcogenides and predicted them to have very useful electronic properties. These simulations have also predicted that monolayers of group IV monochalcogenides will degrade quickly when exposed to water, even in extremely low concentrations. We hypothesize that thin samples of these materials will show signs of degradation if left in air and in water for an extended period of time.

Samples of each of the four monochalcogenides (GeS, GeSe, SnS and SnSe) were exfoliated onto clean oxidized silicon substrates. Chemical analysis showed the SnSe samples were contaminated, so they were excluded from the remainder of the study. The remaining materials were examined optically, topographically, and chemically before and after a 12 hour exposure to water and air. Optical measurements were made with a microscope, chemical characterization was performed with energy dispersive X-ray spectroscopy, and topography was determined with an atomic force microscope. The three measured materials showed no major signs of change after exposure to air or water. While not conclusive, this result has positive implications for the stability of these materials.

Table of Contents

Chapter 1 Introduction

1.1 Piezoelectricity

Certain symmetry breaking materials, when subjected to a mechanical strain, redistribute their internal electric charge in such a way as to produce a net positive charge on one end of the material and a net negative charge on the other end of the material. This charge accumulation is called piezoelectricity. This property of piezoelectric materials is also reversible, allowing for the production of small strains in the material when a voltage is applied (figure 1.1). The ratio of voltage produced to strain applied (or strain produced to voltage applied) is the materials' piezoelectric coefficient.

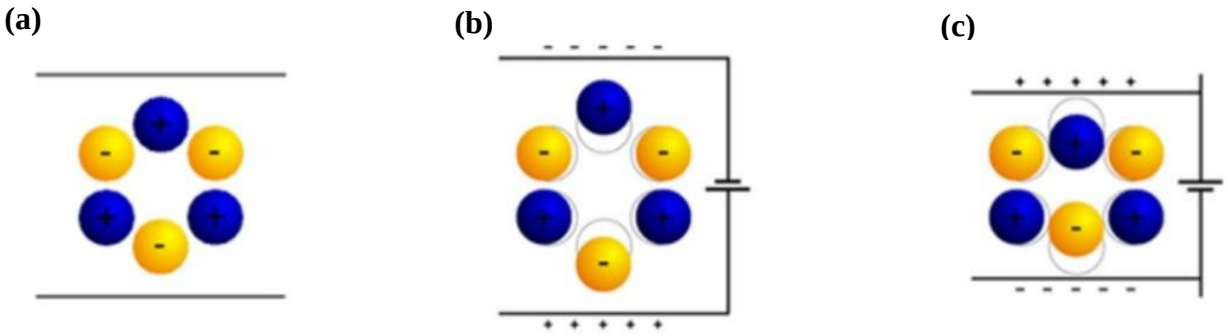

Figure 1.1: (a) Example charge distribution in an unstressed piezoelectric material with no applied voltage. (b) An applied voltage inducing a strain on the material. (c) An opposite voltage inducing an opposite strain on the material [1].

This behavior is observed to some degree in many commonly found materials, such as the quartz crystals used to regulate quartz timepieces, and even human bones [2]. Piezoelectric materials have been an active area of study for over a century, and have had extensive practical applications for almost as long as they have been studied. These applications range from guitar pickups, where they convert strain into voltage, to extremely precise probes, where they convert voltage into strain. The most widely used piezoelectric material is lead zirconate titanate, which

is favored for its high piezoelectric coefficient and relatively low production cost. While this material is currently favored, it and other lead based piezoelectric ceramics still have some drawbacks, most notably the environmental impact of the production of lead based materials, and the disposal of lead based materials [3]. This has led to an increased interest in alternative piezoelectric materials. One area of research for more environmentally friendly materials with high piezoelectric coefficients has been in two dimensional piezoelectrics. These 2D materials tend to have a high capacity for strain, and require very little force to produce a considerable strain. Additionally, these materials take up very little space, allowing for extremely compact practical applications. All of this makes them a promising alternative to lead based bulk piezoelectric materials [4].

1.2 Ferroelectricity

Some piezoelectric materials are also ferroelectric, and allow for spontaneous electric polarization through the application of an external electric field, analogous to ferromagnetic materials formation of a magnetic dipole moment in the presence of an external magnetic field. This electric polarization will remain after the external electric field is removed. This retention of polarization is called hysteresis. This polarity can also be reversed or reoriented through the application of a new electric field with a different direction [5]. Ferroelectric materials are also pyroelectric, meaning polarization can be induced through a change in temperature [6]. Both the temperature and electric field dependence of polarization make ferroelectric materials extremely useful as tunable dielectrics. Ferroelectrics also have applications in laser frequency doubling and optical mixing since they display strong nonlinear optical effects [6].

The property of rewritable polarization and hysteresis also makes ferroelectric materials a potential new source of information storage. An advantage they would have over traditional

magnetic hard drives is that magnetic hard drives require the repeated production of a magnetic field, which requires considerably more power than the production of an electric field. There are two main limitations to the practical application of ferroelectrics; ferroelectric materials lose their polarization when above their curie temperature, which can be below room temperature, and traditional ferroelectric materials only work above a certain minimum size [7]. This size limitation is especially troublesome for their use in information storage.

1.3 Background

Since the discovery of graphene, there has been extensive interest in the properties of 2D materials. Extensive theoretical and experimental research has been done on a number of 2D materials, and recent theoretical work has prompted interest in group IV monochalcogenides. The group IV monochalcogenides (SnSe, SnS, GeSe, GeS) are predicted to have extremely high piezoelectric coefficients [8]. First-principle simulations carried out by Fei et. al. in 2015 showed group IV monochalcogenides to have piezoelectric coefficients one to two times greater then most commonly used 2D or bulk piezoelectric materials [8]. A year later Fei et. al. carried out further simulations and showed that group IV monochalcogenides were ferroelectric as monolayers [9]. While they are not the first 2D materials predicted to be ferroelectric, they are the first that are theorized to be thermally stable at room temperature [9].

While experimental work has shown great potential for these materials, simulations have also implied that group IV monochalcogenides might not be stable under typical conditions (1.3c). Theoretically, monolayers of these materials should fully degrade within nanoseconds when exposed to water under standard temperature and pressure conditions [10].

1.4 Motivation

If monolayer group IV monochalcogenides have both strong piezoelectric and ferroelectric properties, they could have extensive practical applications. Their size, strength, and high piezoelectric coefficient would let them be an improvement to many existing applications of piezoelectrics. Their ferroelectric properties could lead to whole new technologies. As discussed earlier, the major drawback of ferroelectric materials in information storage was their stability at room temperature and their size, but group IV monochalcogenides would potentially solve both of those problems.

Since the theoretical applications of these materials are extensive, fabrication of 2D group IV monochalcogenides could be of considerable importance. Fabrication of 2D materials often necessitates brief or extended periods of exposure to atmospheric conditions, and there is reason to believe such conditions could degrade group IV monochalcogenides [10]. As such, it is important to know in practice how samples of these materials react to water containing environments, to determine if fabrication of these materials is feasible if there is exposure to moisture.

1.5 Organization

Chapter 2 will cover the substrate preparation process, the mechanical exfoliation methods used to produce thin samples of group IV monochalcogenides, and the attempts made to reduce the thickness of flakes through nitrogen etching. Chapter 3 will cover the chemical characterization of the group IV monochalcogenides before and after exposure to water and air. Chapter 4 will describe the topographical measurements made through atomic force microscopy and optical imaging before and after exposure. A summary of the work done will then be covered in chapter 5 along with a discussion of potential future work.

Chapter 2 Sample Preparation

2.1 Crystal growth

Small sample crystals of each of the four group IV monochalcogenides were obtained from sources that grew them using chemical vapor transport. Chemical vapor transport is a method of crystal growth that involves heating a stoichiometric mixture of elements that make up the desired crystal in the hotter end of a container with a stark temperature gradient [11, 12]. These heated precursor elements are volatilized in the presence of a gaseous reactant referred to as a transport agent. In the case of group four monochalcogenides, this is usually a halogen or halogen compound, such as iodine [13]. The volatilized precursor elements are circulated with the transport agent toward the cooler end of the container where the precursor elements will cooldown and reform as the desired crystal compound [11, 12]. A diagram of this process from Ref. [11] is given in Figure 2.1.

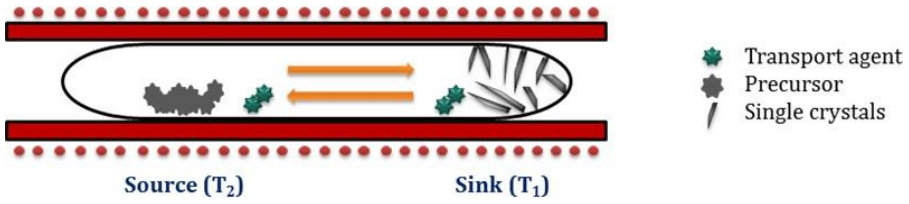

Figure 2.1: Diagram of chemical vapor transport process for components at a high temperature zone (T_2) to crystals at a low temperature zone (T_1) [11].

2.2 Substrate preparation

A large silicon substrate with a 300 nm thermal oxide layer was scored with a metal scribe, and broken along the score to produce roughly 0.5 cm by 0.5 cm square chips of substrate. These chips were then cleaned by being sonicated in acetone for 3 minutes and then rinsed in isopropyl alcohol, and blown dry with pressurized nitrogen while in a fume hood. These chips were then treated with oxygen plasma for 30 seconds to further remove organic

contaminants and improve adhesion to the crystals. These chips were then transferred to a nitrogen filled glovebox for storage until they were exfoliated on.

2.3 Exfoliation

2.3.1 Traditional exfoliation

The bulk samples of group IV monochalcogenides were stored in the nitrogen filled glove box. These bulk samples were each exfoliated onto prepared substrates. Three different methods of exfoliation were compared: traditional exfoliation, heated exfoliation, and gold mediated exfoliation. These exfoliation processes were done in the glovebox. Disposable gloves were placed over the glovebox gloves, and a wax paper mat was placed down for this process. These were disposed of and replaced between exfoliating each of the four materials in order to prevent contamination of samples. Similarly the tweezers were wiped down after each use.

For traditional exfoliation, each bulk crystal was placed on semiconductor wafer dicing tape with tweezers. They were then removed, leaving behind a small layer of crystal on the tape. The tape was then folded in half, to press the small layer of crystal to another section of tape. The tape was then unfolded, leaving some of the small layer of crystal on the new section of tape. This process was repeated several times until much of the tape was covered in a very thin layer of crystal. The tape was then pressed to a prepared substrate chip and peeled off in order to leave behind very thin samples of the crystal.

2.3.2 Heated exfoliation

Heated exfoliation involved the same process as traditional exfoliation, except after the tape was pressed to the prepared substrate chip, the chip and the tape were heated before the tape was removed. They were placed on a hot plate at 120 ℃ for 2.5 minutes, then the tape was removed [14, 15]. This process has been tried on other 2D materials and has been shown to

weaken the bonds between the layers of the crystal flakes on the tape resulting in thinner flakes being transferred to the substrate. It also allows for the improved adhesion of flakes to substrates, and provides wider flakes in greater numbers [14, 15].

2.3.3 Gold mediated exfoliation

The bond strength of gold to transition metal dichalcogenides has been experimentally shown to be stronger than the bond strength of SiO_2 substrates with transition metal dichalcogenides [16]. Because of this greater bond strength, more material will be attached to a layer of gold peeled off the exfoliating tape than would be attached to a substrate after traditional exfoliation. Since all of the material attached to the gold can be transferred to the substrate, gold mediated exfoliation yields better results than traditional exfoliation of transition metal dichalcogenides [16].

Gold mediated exfoliation is a method used in Ref. [16] to obtain more flakes with greater width. For gold mediated exfoliation, gold was evaporated onto the tape after it had been folded repeatedly to produce thin samples of the crystal. Samples were prepared with three different thicknesses of gold: 40 nm, 80 nm, and 150 nm. Thermal release tape was then pressed to the gold and peeled off. When the thermal release tape was peeled off it would take with it the layer of gold, and the gold would take with it a thin layer of crystal. The crystal, gold, and thermal release tape would then be pressed to a prepared substrate. This was then placed on a hot plate at 100 ^{o}C until the release tape lost its adhesion to the gold. The substrate was then removed from the glovebox and immediately placed into a gold etching solution of potassium iodide until the gold layer had been removed. Figure 2.2 outlines the process.

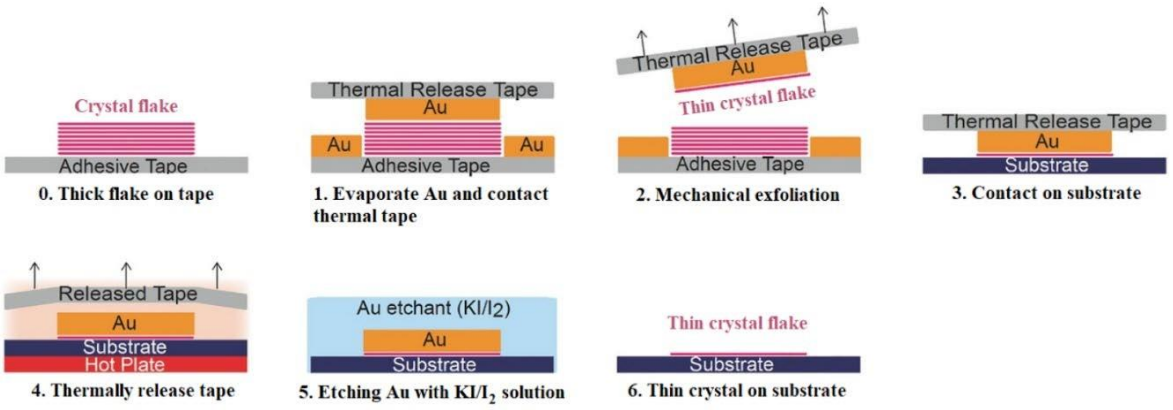

Figure 2.2: Illustration of gold mediated exfoliation process. Modified from [16].

Once the gold had been removed, the substrate was placed in acetone and then IPA to remove excess gold etch and tape residue. Excess IPA was then blown off the sample with compressed nitrogen. The sample was then returned to the glovebox. Care was taken in these steps to minimize exposure to air.

2.3.4 Exfoliation comparison

After all three methods of exfoliation were attempted; they were compared to see which would be the most suitable for use in the rest of the study. Since the theoretical work on the degradation of group IV monochalcogenides examined only monolayers, the primary metric by which the exfoliation methods were compared was flake thickness. Flake thickness was also of foremost concern because if degradation resulted in a decrease in thickness by some fixed amount, it would be more easily observed on thin flakes, since it would be a greater percentage of the flakes total thickness. Relative thickness of flakes was optically determined by the color of the flakes, thicker flakes being a brighter yellow color, while thinner flakes range from a duller yellow, to a red, to a green, and then to a light blue when extremely thin. Additional metrics that were considered were flake yield, flake width, and the cleanliness of the substrate surrounding the flakes.

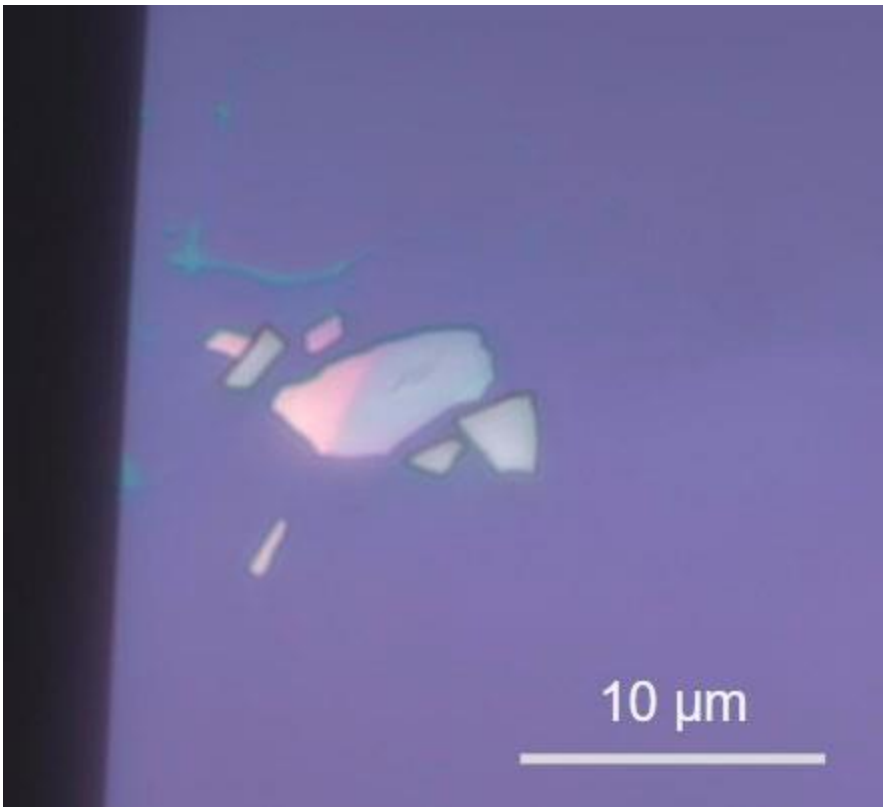

Figure 2.3: Example GeSe flakes. The central largest flake decreases in thickness from left to right as indicated by the color change. A green line of glue left from exfoliation can be seen above the flakes, but most of the surrounding substrate is clean.

Once flakes had been exfoliated onto substrates, the substrates were placed into hermetically sealed transfer cells. These cells ensured that the samples would not be exposed to air. Then they were removed from the glovebox, and their compact design and glass window allowed for imaging under microscopes without the need for any modifications to the microscope [15]. After safe removal from the glovebox, samples produced by each exfoliation method were examined under an optical microscope at magnifications of 5x, 20x, 50x, and 100x. The three methods of gold exfoliation were compared, and while 40 nm of gold seemed to produce the worst results, little difference was seen between the 80 nm and 150 nm samples. After the three methods of gold exfoliation were compared, the best forms of gold exfoliation were compared with traditional and heated exfoliation. Figure 2.5 shows a comparison of

representative samples of each method. Due to a superior flake yield, heated exfoliation was chosen for sample preparation.

Figure 2.4: A sealed transfer cell containing a substrate secured in place by black carbon tape.

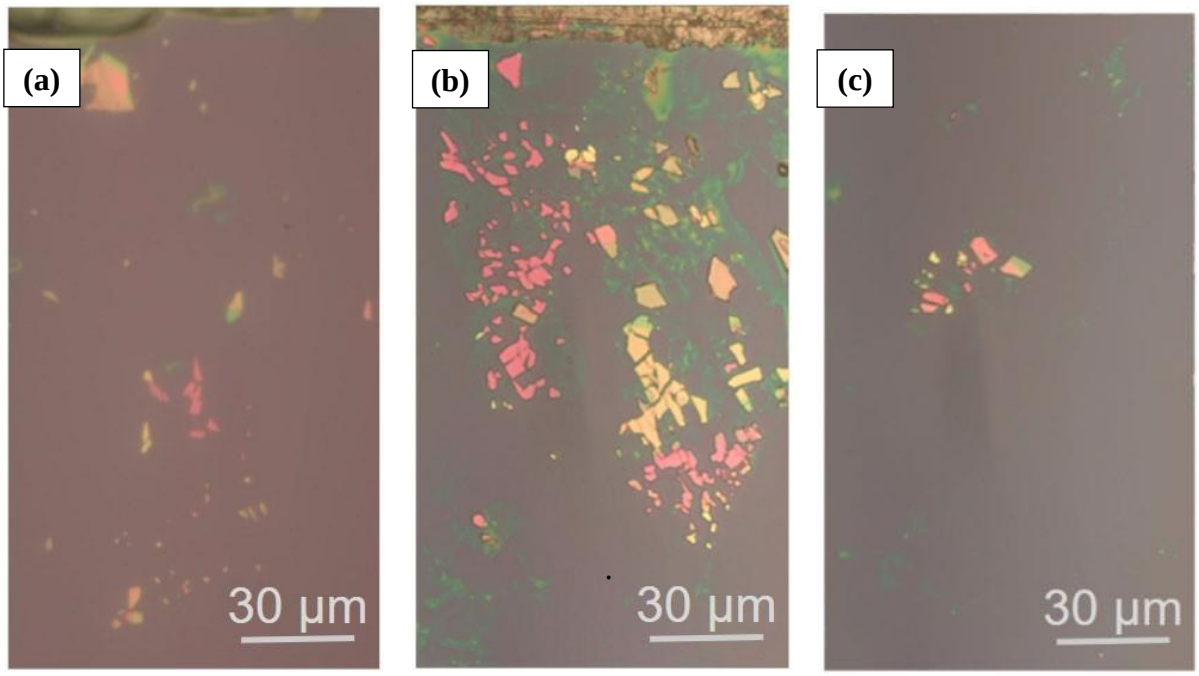

Figure 2.5: Results from (a) traditional, (b) heated, and (c) gold mediated exfoliation.

2.4 Nitrogen etching

Once the optimum form of exfoliation was chosen, an attempt was made to further improve samples by reducing their thickness through nitrogen etching, a process outlined in Ref. [17]. Samples were placed in a quartz boat at the cool end of a quartz tube while the center of the tube was heated to 700 ºC over the course of 20 minutes. The boat was then pulled into the center of the quartz tube and left there for 20 minutes while N_2 was circulated through the tube at 50 sccm. The pulling process was achieved by attaching a metal chain to the boat, and running the chain down the length of the tube. After the 20 minutes of initial heating a magnet was placed against the outside of the tube and used to drag the chain, moving the boat into the heating zone.

Figure 2.6: Tube furnace with a quartz boat on the left end and a chain running from the boat to the right end of the tube.

Several variations of this process were also tried, ranging the temperature from 600 ºC to 800 ºC, and ranging the time from 15 minutes to 2 hours. When the samples were done heating they were left in the quartz chamber to cool down. Once cooled, they were removed and quickly transferred to the glovebox to minimize exposure to air. They were then placed inside the sealed cells and removed from the glovebox to be imaged.

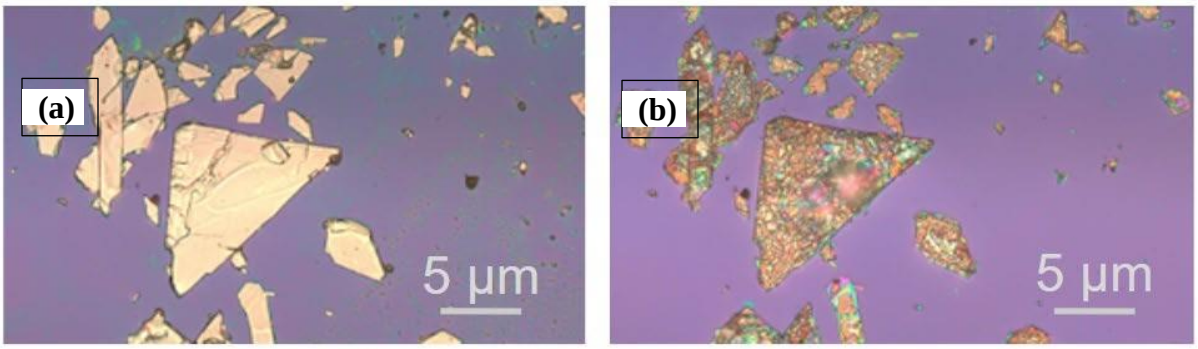

Figure 2.7: SnS flakes (a) before and (b) after nitrogen etching.

Imaging showed that neither the original process, nor any variations, produced better samples. Since nitrogen etching caused considerable damage to the flakes, it was not performed on future samples.

2.5 Flake exposure

Heated exfoliation was used to produce several substrates with samples of each material. These samples were not nitrogen etched. The substrates were then removed from the glovebox in the sealed cells. The entirety of each substrate was then examined under the microscope and the thinnest flakes found with clean surrounding substrate were imaged and cataloged. The cells would then be unsealed and returned to the glovebox. Any time a sample was returned to the glovebox it would be placed in the glovebox antechamber and the antechamber would be sealed and pumped down below 750 Torr for three minutes. The antechamber would then be filled with nitrogen and pumped down again. This process was done three times before moving the cell from the antechamber into the main chamber of the glovebox.

To expose flakes, samples were left in air and in water for 12 hours. Samples exposed to air were removed from the glovebox and left in non-airtight containers for 12 hours and then returned to the glove box. Samples exposed to water were removed from the glove box while in sealed cells. These cells were then opened under the surface of water that had been boiled and

then allowed to return to room temperature. Samples were left in the water for 12 hours before being removed, rinsed in acetone then IPA, blown dry with compressed nitrogen, and returned to the glovebox.

Chapter 3 Chemical Characterization

3.1 Energy dispersive X-ray spectroscopy

Chemical analysis of each of the four materials was performed before and after exposure using energy dispersive X-ray spectroscopy (EDX). EDX is a method of chemical characterization that uses a scanning electron microscope (SEM) to excite the surface layers of a material with an electron beam [18]. The surface layers will then emit x-rays with wavelengths specific to their atomic structure [18]. These emitted x-rays are then analyzed with an energy dispersive detector, a solid state device built into the SEM that can distinguish x-ray wavelengths [18].

3.2 Measuring process

Substrates with each material were taken to an SEM while in sealed cells. They were then removed from the cells and placed into the SEM. The pressure inside the SEM was then reduced to 10^{-4} Torr. The imaging function of the SEM was then used to search the substrate for flakes. Once a flake was found it was examined using EDX. ESPRIT microanalysis software was then used to convert raw spectroscopy data into relative atomic weights and percentages. Since there exists some overlap between wavelength peaks for different elements, the software was told to look for Si, O, and C in addition to the two elements in the group IV monochalcogenides that was being examined. This allowed the software to break up overlapping regions into two parts, attributing some of the intensity to one element, and some of the intensity to the other element. Si, O, and C were chosen because they were the elements observed when EDX analysis was

performed on blank regions of the substrate. These elements were still present in EDX analysis of flakes because the flakes were thin enough that some percentage of the electron beam was able to travel all the way through the flake and then be absorbed by the substrate.

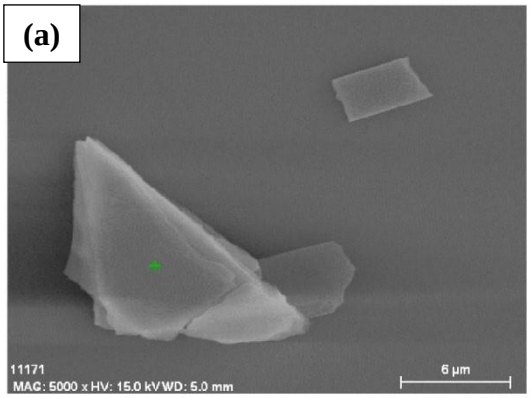

(b)

El	norm. C [wt.%]	Atom. C [at.%]	Error (1 Sigma) [wt.%]
C	12.82	45.72	2.78
O	2.01	5.37	0.58
Si	0.62	0.95	0.06
S	17.89	23.90	0.58
Sn	66.67	24.06	1.76

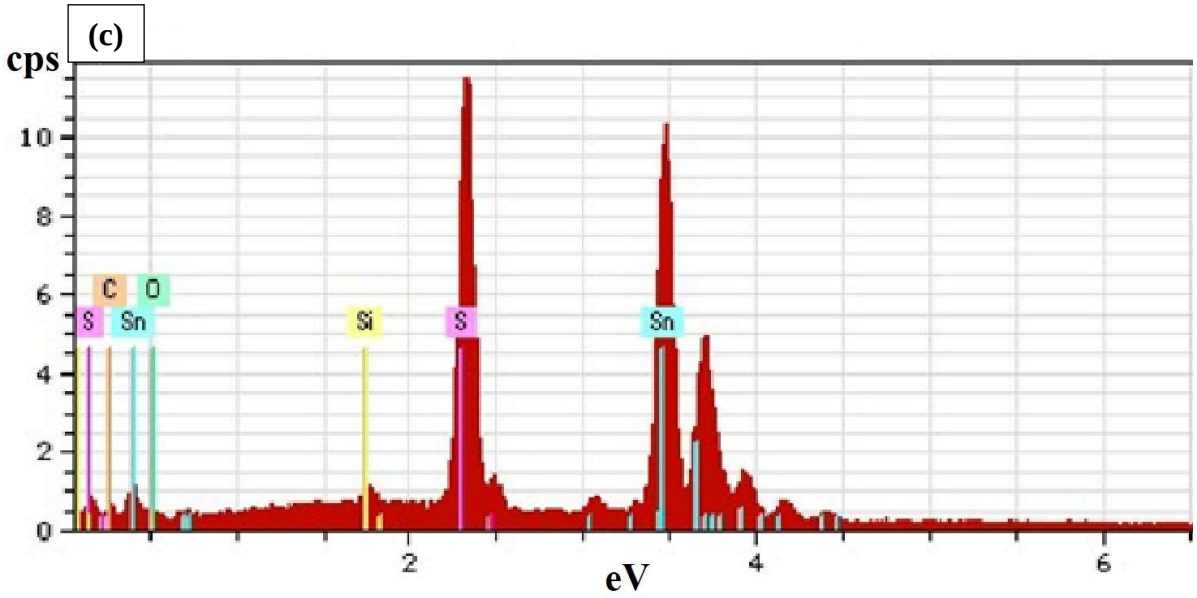

Figure 3.1: (a) SEM image of a typical SnS flake. The green cross indicates where elemental composition was measured. (b) Relative weight [wt. %] and number of atoms [at. %] for selected elements, along with the 1 sigma error for relative weights. (c) Emitted x-ray energy graph for the same flake showing the counts per second of x-rays of different energies.

3.3 Analysis and comparison

Ten flakes of each material were analyzed and the mean ratio of elements was calculated for each material. The expected mean was 1, since all group IV monochalcogenides are

composed of equal parts of two elements. Samples of GeS, GeSe, and SnS were all consistently near the expected mean, all with ratios close to 1, and standard deviations less than 0.1. Ratios of SnSe were not consistently near 1. The mean ratio of Sn to Se was 0.6395, and the standard distribution was 0.8085.The cause of the inconsistency was not clear. It was possibly the result of an impure starting bulk crystal, contamination during the exfoliation process, or rapid degradation in the moments it spent exposed to air. Since SnSe samples could not be consistently obtained, they were excluded from further analysis.

10 flakes of GeS, GeSe and SnS were exposed to air, and another 10 to water. The mean ratios and standard deviations of those ratios were calculated as before, and compared to pre exposed samples (Figure 4.2). These materials showed no significant change in observed composition after exposure to air or water.

Material	**Pre Exposure**		**Air Exposure**		**Water Exposure**	
	Mean	**Std. Dev**	**Mean**	**Std. Dev**	**Mean**	**Std. Dev**
GeS	**0.9232**	**0.0684**	**0.9422**	**0.0548**	**1.012**	**0.0621**
SnSe	**1.0606**	**0.0531**	**0.9801**	**0.0601**	**1.0204**	**0.0554**
SnS	**1.0452**	**0.0917**	**1.0224**	**0.0722**	**0.9867**	**0.0692**

Figure 3.2: Table of mean ratios of elements and standard deviations of ratios for 10 samples of each material before exposure, after exposure to air, and after exposure to water.

Chapter 4 Topographical Measurements

4.1 Introduction

Degradation of 2D materials is most commonly apparent from a change in topography. This change is typically a decrease in thickness and/or the formation of blisters on the surface of the material. This is observed in black phosphorus, a material of interest because it is isoelectronic with group IV monochalcogenides and shares the same crystal symmetries [19, 20]. Since black phosphorus has many of the same properties as the group IV monochalcogenides, its degradation behaviors were researched to serve as a comparison.

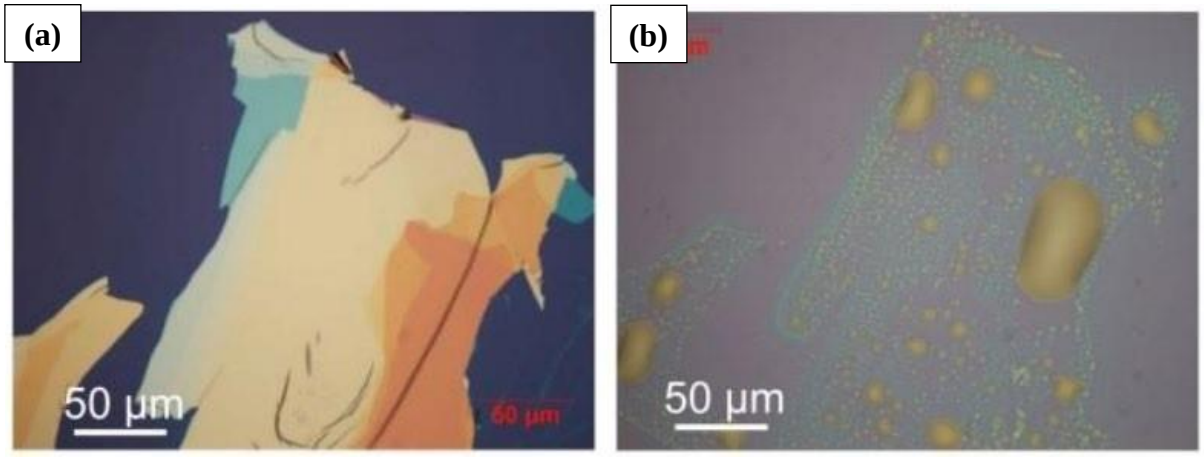

Figure 4.1: Optical images of black phosphorus before and after oxidation from Ref. [21].

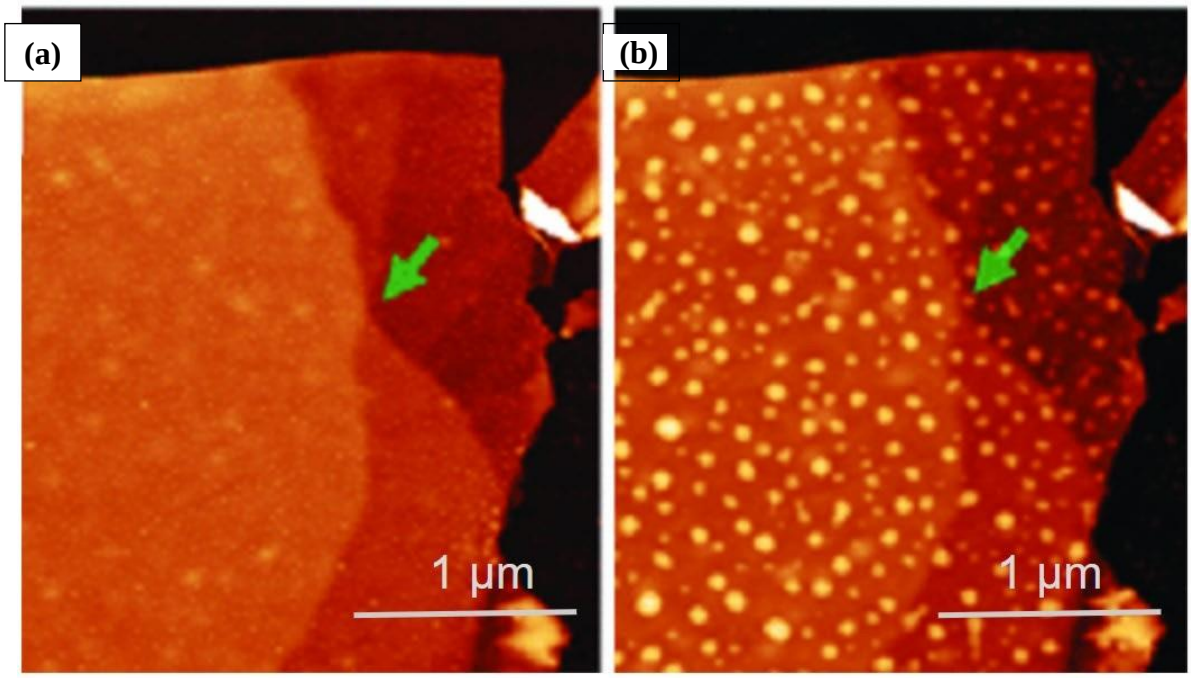

Figure 4.2: Atomic force microscopy height images from Ref. [22] of black phosphorus before and after oxidation. An example blister formation is indicated by the green arrow.

4.2 Atomic force microscopy

Flakes were examined using an atomic force microscope (AFM) in order to obtain quantitative measurements of their thicknesses. The AFM uses an extremely small tip at the end of a reflective cantilever to scan the surface of a material. The cantilever oscillates as it moves over the scanning region, and a laser is bounced off the cantilever onto a photodiode. When the tip approaches the surface during its oscillation, it is deflected somewhat by Van Der Waals forces and electrostatic forces between the tip and the surface. These forces result in a change in oscillation amplitude. Since the strength of these forces depends on distance, the closer the surface is to the tip, the greater the change in oscillation amplitude. The photodiode measures the change in amplitude for each tip location, and based on that change in amplitude the height of each location is determined. By doing this repeatedly as the tip moves across a surface the AFM produces a topological map of the scanned region.

4.3 Topographical comparison

Optical and AFM images were taken of several flakes of each of the three materials of interest before and after exposure to water and air. A few representative flakes for each material are shown below in Figs. 4.3 through 4.8. The oxidation behavior of black phosphorus shown in Fig. 4.1 and 4.2 was not observed in any of the exposed materials.

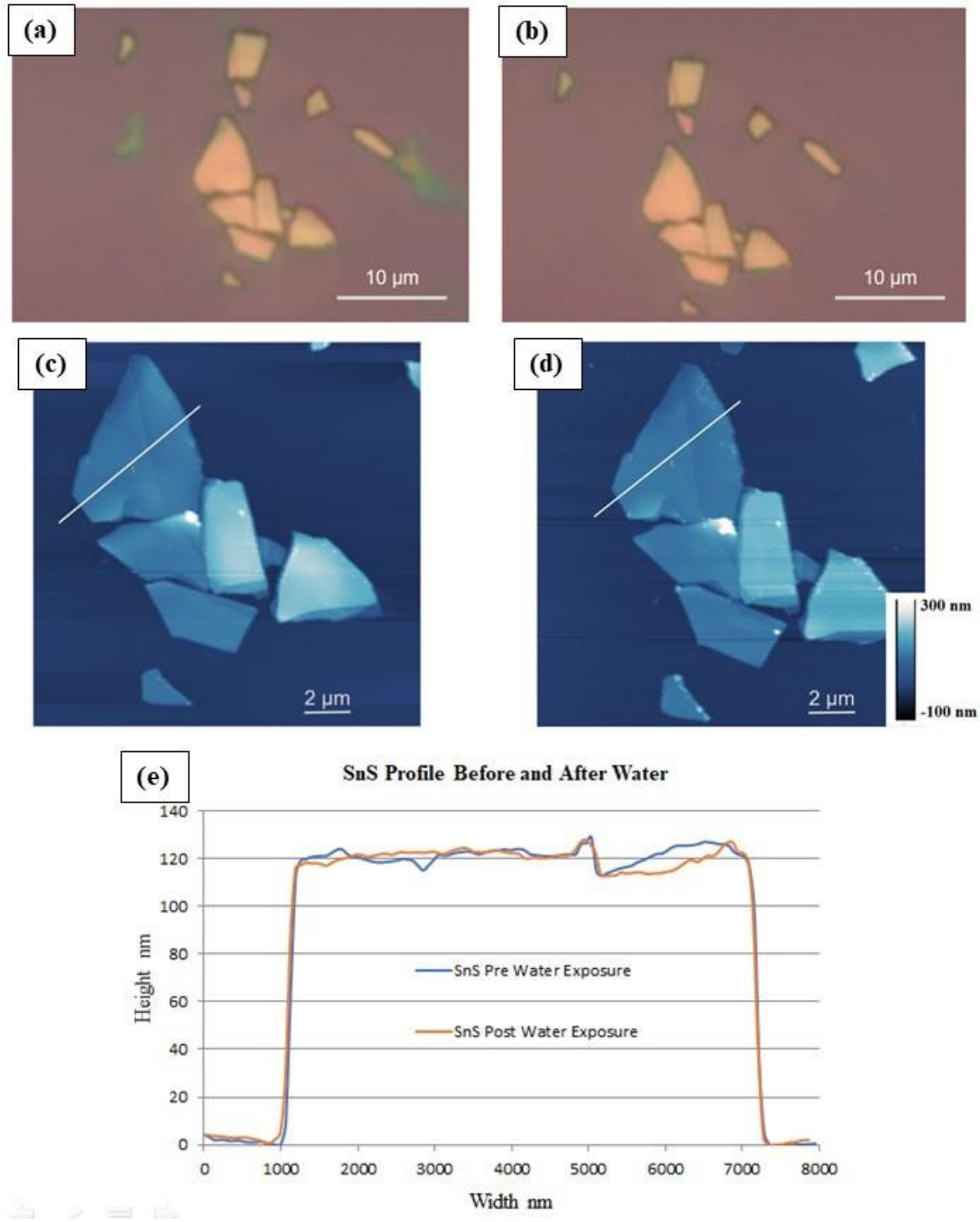

Figure (4.3) Optical images of SnS (a) before and (b) after exposure to water. AFM images of the same flakes (c) before and (d) after exposure to water. (e) Overlaid height profiles of SnS along the white lines in (c) and (d).

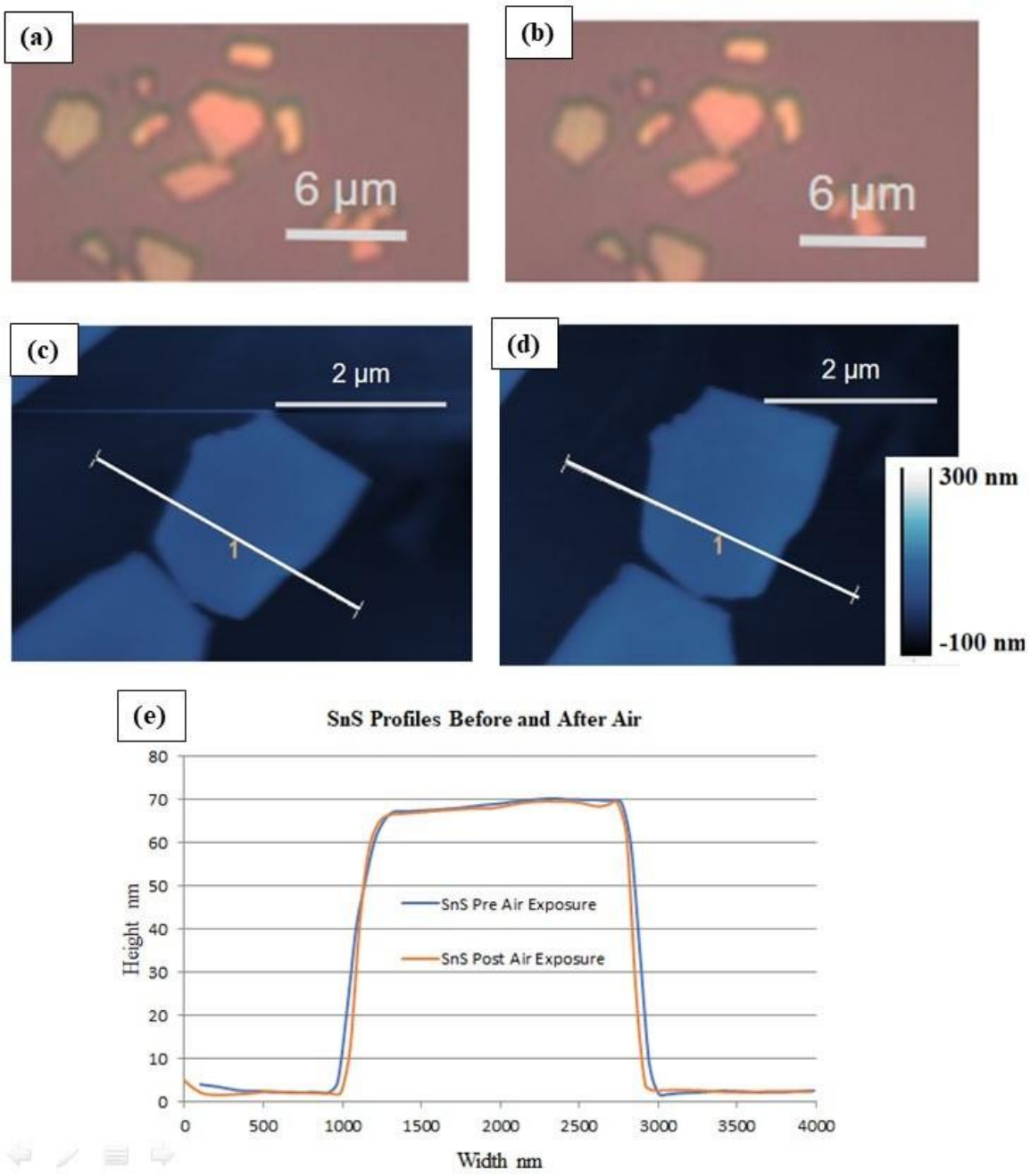

Figure (4.4) Optical images of SnS (a) before and (b) after exposure to air. AFM images of the same flakes (c) before and (d) after exposure to air. (e) Overlaid height profiles of SnS along the white lines in (c) and (d).

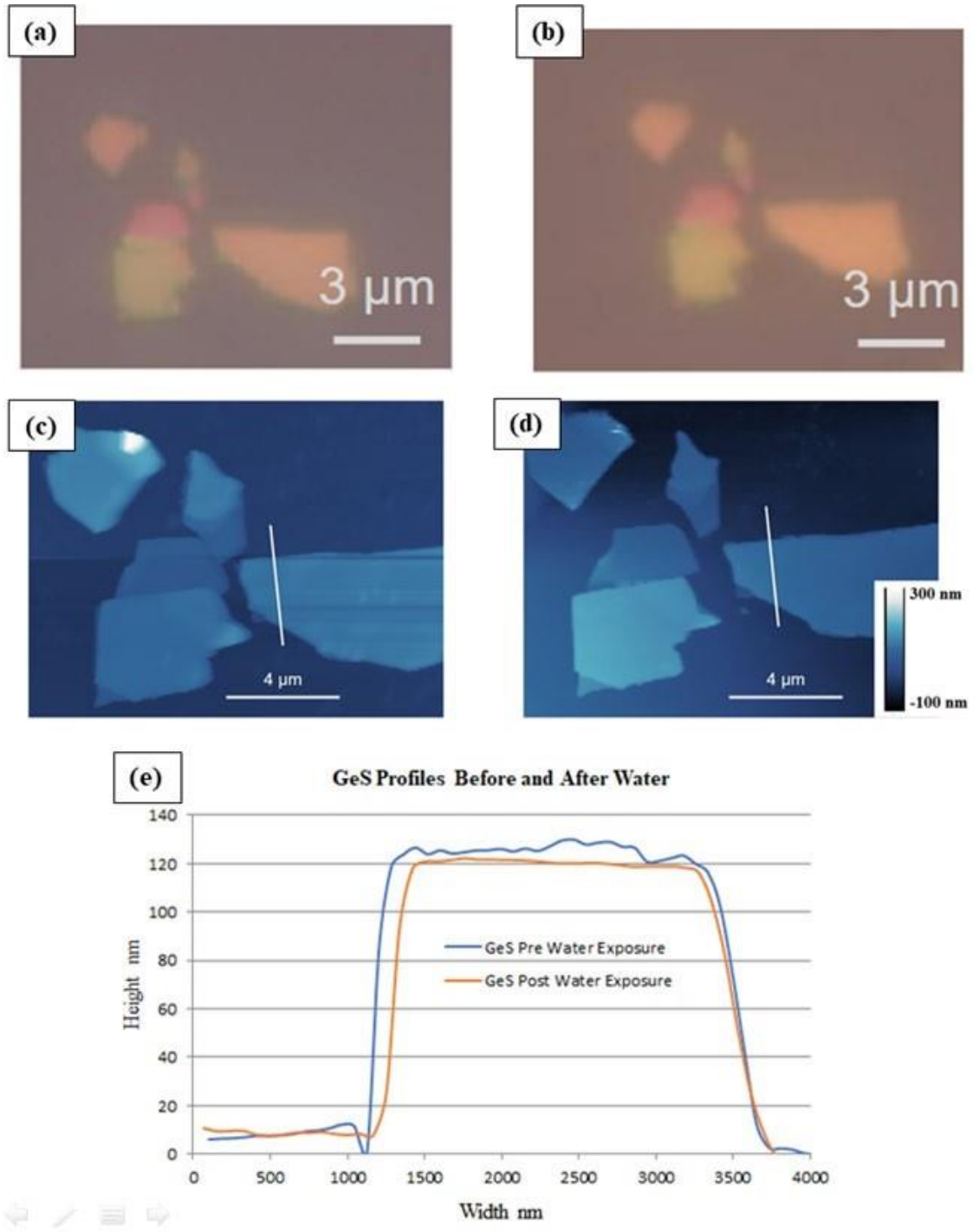

Figure (4.5) Optical images of GeS (a) before and (b) after exposure to water. AFM images of the same flakes (c) before and (d) after exposure to water. (e) Overlaid height profiles of GeS along the white lines in (c) and (d).

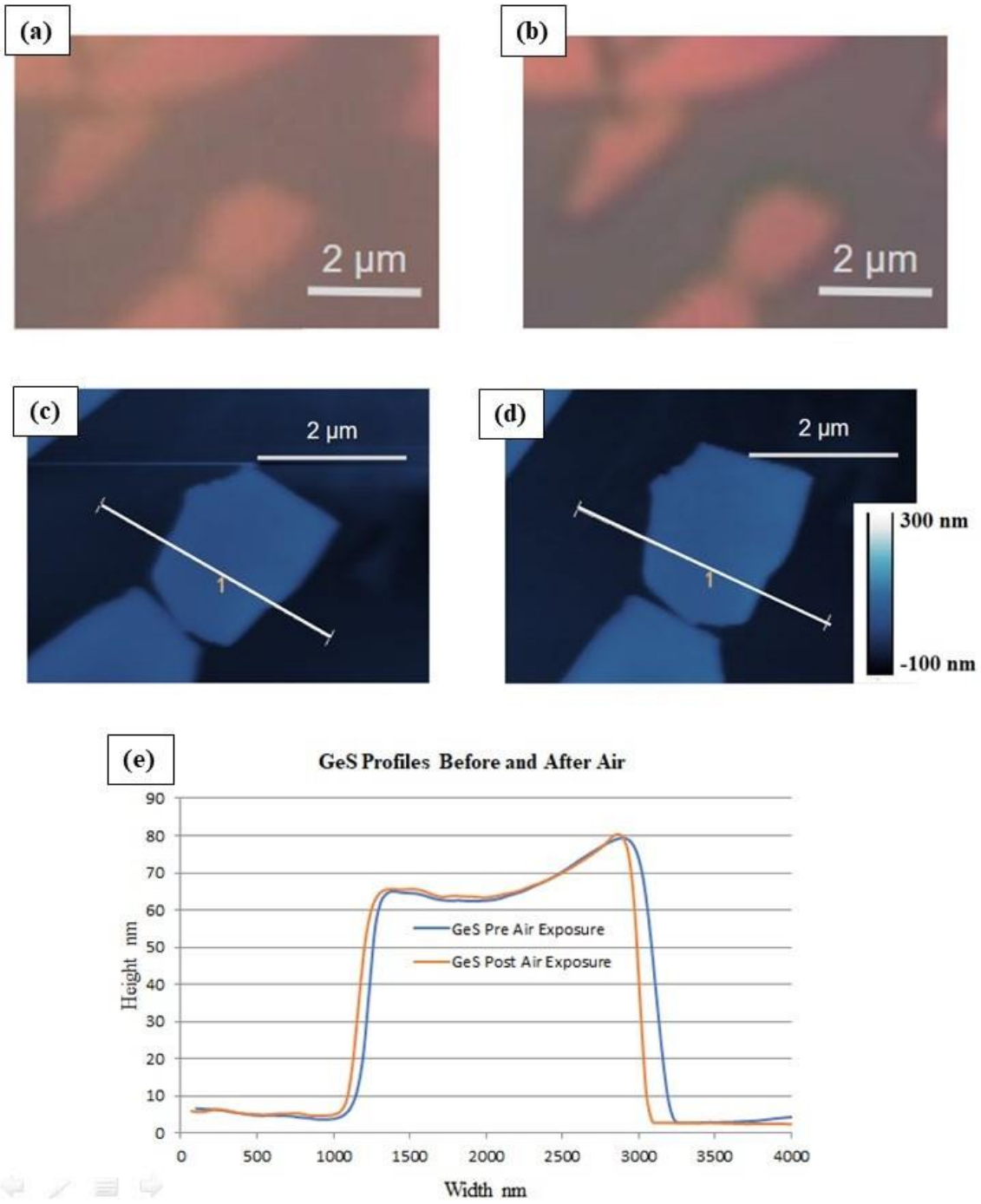

Figure (4.6) Optical images of GeS (a) before and (b) after exposure to air. AFM images of the same flakes (c) before and (d) after exposure to air. (e) Overlaid height profiles of GeS along the white lines in (c) and (d).

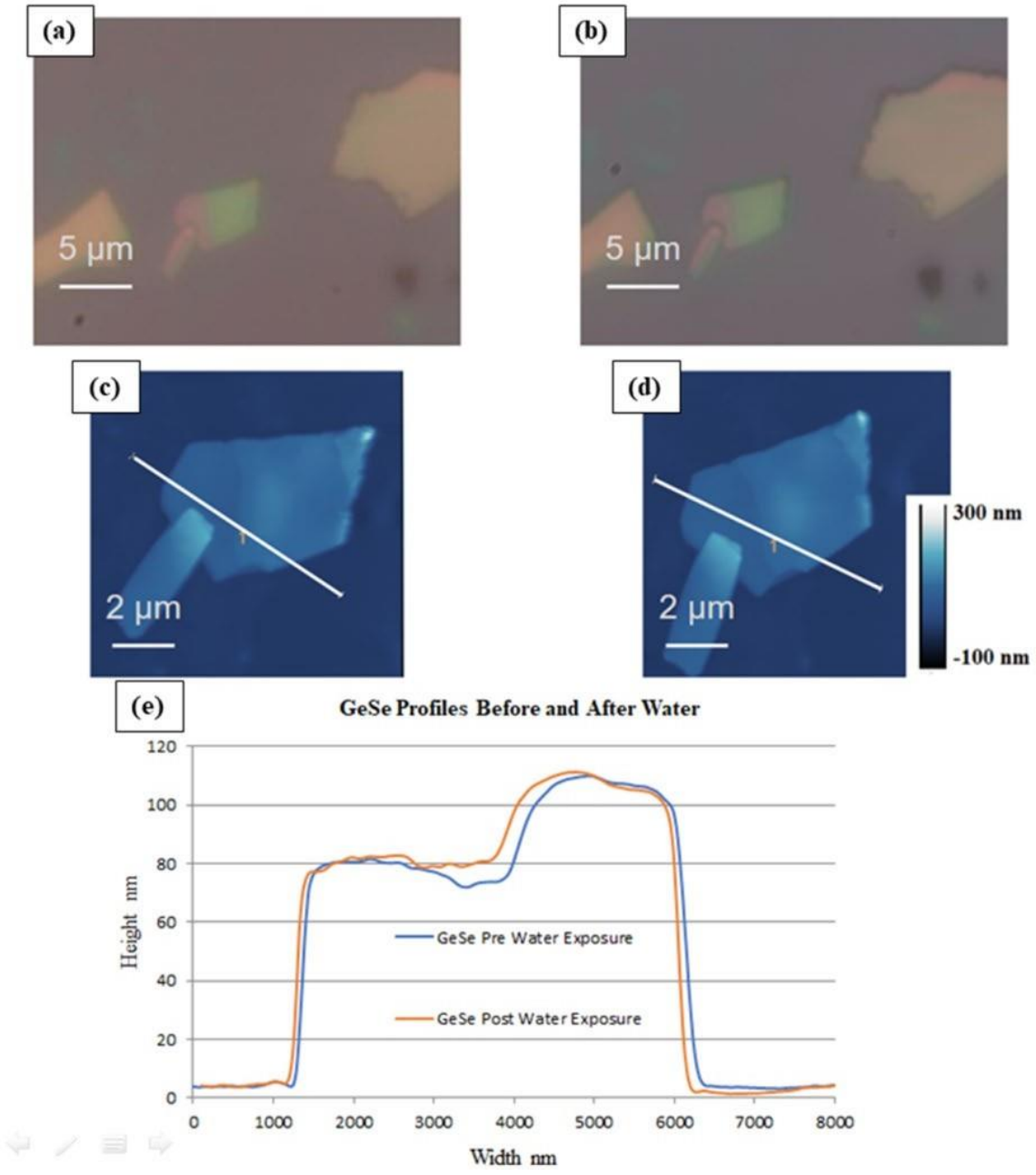

Figure (4.7) Optical images of GeSe (a) before and (b) after exposure to water. AFM images of the same flakes (c) before and (d) after exposure to water. (e) Overlaid height profiles of GeSe along the white lines in (c) and (d).

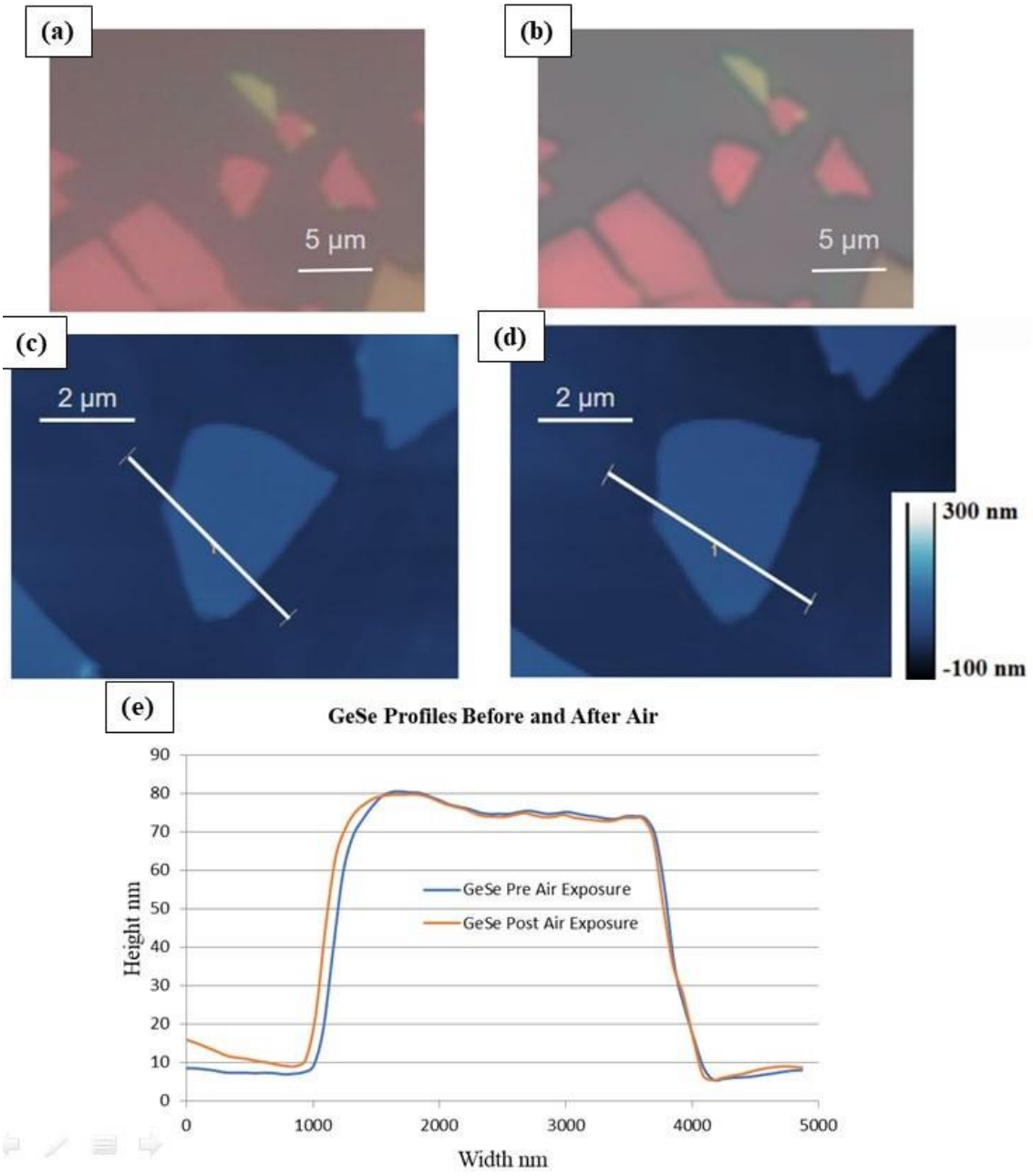

Figure (4.8) Optical images of GeSe (a) before and (b) after exposure to air. AFM images of the same flakes (c) before and (d) after exposure to air. (e) Overlaid height profiles of GeSe along the white lines in (c) and (d).

Chapter 5 Summary and Future Work

5.1 Summary

Theoretical models of group IV monochalcogenides have suggested they possess several useful traits when extremely thin. Similarly, models have predicted that they could be extremely sensitive to water, even at levels found in air. Since a sensitivity could be a hindrance to future work, an attempt was made to experimentally quantify their reaction to air and water. To do this, samples of each material were exfoliated onto cleaned SiO_2 substrates. Traditional, heated, and gold mediated exfoliation methods were tried, and heated exfoliation was found to produce the best results. Nitrogen etching was used to reduce flake thickness, but it led to considerable flake degradation so it was not continued. Once several substrates were exfoliated with each material, flakes on those substrates were imaged optically. After imaging, the chemical composition of the samples was determined using EDX. This process showed that the samples that were expected to be SnSe were contaminated, or in some way degraded. Because of this, SnSe was not included in further measurements. Samples were then exposed to water and air for 12 hours. After exposure EDX was used to determine any change in elemental composition, but no changes were observed. An AFM was used to take topographical measurements of samples before and after exposure to water and air, but again, no significant changes were observed.

5.2 Future work

No clear signs of degradation were found in GeS, GeSe, or SnS, and no post exposure measurements of SnSe were able to be made. Clearly further attempts can be made to exfoliate SnSe flakes devoid of contamination. Additionally, while considerable effort was made to produce thin flakes of each material, no monolayers were achieved. Further work could then be done to produce monolayers, so that experimentation can more closely represent the theoretical

modeling of monolayers. Another route for future experimentation would be increased time scales. Samples exposed for 12 hours did not show signs of degrading, but perhaps longer exposures would have yielded different results.

References

[1] Piezoelectricity. (n.d.). Retrieved July 7, 2018, from https://education.mrsec.wisc.edu/piezoelectricity/

[2] Fukada, E., & Yasuda, I. (1957). On the Piezoelectric Effect of Bone. Journal of the Physical Society of Japan, 12(10), 1158-1162. doi:10.1143/jpsj.12.1158

[3] Kimura, M., Ando, A., & Sakabe, (2010). Lead zirconate titanate-based piezo-ceramics. .Japan: Murata Manufacturing Co., Ltd.

[4] Fei, R., Li, W., Li, J., & Yang, L. (2015). Giant piezoelectricity of monolayer group IV monochalcogenides: SnSe, SnS, GeSe, and GeS. Applied Physics Letters, 107(17), 173104. doi:10.1063/1.4934750

[5] AZoM. (2006, November 21). Ferroelectric Material - Properties and Applications of Ferroelectric Materials. Azom. https://www.azom.com/article.aspx?ArticleID=3593

[6] Müller, J., Böscke, T. S., Schröder, U., Mueller, S., Bräuhaus, D., Böttger, U., Frey, L., & Mikolajick, T. (2012). Ferroelectricity in Simple Binary ZrO2 and HfO2. Nano Letters, 12(8), 4318–4323. https://doi.org/10.1021/nl302049k

[7] Whatmore R. (2017) Ferroelectric Materials. In: Kasap S., Capper P. (eds) Springer Handbook of Electronic and Photonic Materials. Springer Handbooks. Springer, Cham. https://doi.org/10.1007/978-3-319-48933-9_26

[8] Fei, R., Li, W., Li, J., & Yang, L. (2015). Giant piezoelectricity of monolayer group IV monochalcogenides: SnSe, SnS, GeSe, and GeS. Applied Physics Letters, 107(17), 173104. https://doi.org/10.1063/1.4934750

[9] Fei, R., Kang, W., & Yang, L. (2016). Ferroelectricity and Phase Transitions in Monolayer Group-IV Monochalcogenides. Physical Review Letters, 117(9), 1–3. https://doi.org/10.1103/physrevlett.117.097601

[10] Barraza-Lopez, S., & Kaloni, T. P. (2018). Water Splits To Degrade Two-Dimensional Group-IV Monochalcogenides in Nanoseconds. ACS Central Science, 4(10), 1436–1446. https://doi.org/10.1021/acscentsci.8b00589

[11] Shekhar, C. S. (n.d.). Chemical vapor transport. Max Planck Institute for Chemical Physics of Solids. Retrieved October 26, 2020, from https://www.cpfs.mpg.de/2651362/chemical-vapor-transport#:%7E:text=Chemical%20vapour%20transport%20(CVT)%2C,include%20halogens%20and%20halogen%20compounds

[12] Ferreira, S. (2013). Advanced Topics on Crystal Growth. IntechOpen. https://doi.org/10.5772/55547

[13] Murgatroyd, P. A. E., Smiles, M. J., Savory, C. N., Shalvey, T. P., Swallow, J. E. N., Fleck, N., Robertson, C. M., Jäckel, F., Alaria, J., Major, J. D., Scanlon, D. O., & Veal, T. D.

(2020). GeSe: Optical Spectroscopy and Theoretical Study of a van der Waals Solar Absorber. Chemistry of Materials, 32(7), 3245–3253. https://doi.org/10.1021/acs.chemmater.0c00453

[14] Huang, B., Clark, G., Navarro-Moratalla, E., Klein, D. R., Cheng, R., Seyler, K. L, X. (2017). Layer-dependent ferromagnetism in a van der Waals crystal down to the monolayer limit. Nature, 546(7657), 270-273. doi:10.1038/nature22391

[15] Thompson, J. P., Doha, M. H., Murphy, P., Hu, J., & Churchill, H. O. H. (2019). Exfoliation and Analysis of Large-area, Air-Sensitive Two-Dimensional Materials. Journal of Visualized Experiments, 143, 1–3. https://doi.org/10.3791/58693

[16] Desai, S. B., Madhvapathy, S. R., Amani, M., Kiriya, D., Hettick, M., Tosun, M., Zhou, Y., Dubey, M., Ager, J. W., Chrzan, D., & Javey, A. (2016). Gold-Mediated Exfoliation of Ultralarge Optoelectronically-Perfect Monolayers. Advanced Materials, 28(21), 4053–4058. https://doi.org/10.1002/adma.201506171

[17] Jiang, J., Wong, C. P. Y., Zou, J., Li, S., Wang, Q., Chen, J., Qi, D., Wang, H., Eda, G., Chua, D. H. C., Shi, Y., Zhang, W., & Wee, A. T. S. (2017). Two-step fabrication of single-layer rectangular SnSe flakes. 2D Materials, 4(2), 021026. https://doi.org/10.1088/2053-1583/aa6aec

[18] Narayan, R. (2016). Monitoring and Evaluation of Biomaterials and their Performance In Vivo (1st ed., Vol. 4). Woodhead Publishing. https://doi.org/10.1016/C2014-0-04050-6

[19] Xia, F., Wang, H., Hwang, J. C. M., Neto, A. H. C., & Yang, L. (2019). Black phosphorus and its isoelectronic materials. Nature Reviews Physics, 1(5), 306–317. https://doi.org/10.1038/s42254-019-0043-5

[20] Gomes, L. C., Carvalho, A., & Castro Neto, A. H. (2016). Vacancies and oxidation of two-dimensional group-IV monochalcogenides. Physical Review B, 94(5), 1–2. https://doi.org/10.1103/physrevb.94.054103

[21] Huang, Y. et al. Degradation of black phosphorus (BP): the role of oxygen and water. Preprint at http://arxiv.org/abs/1511.09201 (2015).

[22] Wood, J. D., Wells, S. A., Jariwala, D., Chen, K.-S., Cho, E. K., Sangwan, V. K., Liu, X., Lauhon, L. J., Marks, T. J., & Hersam, M. C. (2014). Effective Passivation of Exfoliated Black Phosphorus Transistors against Ambient Degradation. Nano Letters, 14(12), 6964–6970. https://doi.org/10.1021/nl5032293